Inorg. Chem. **2007**, *46*, 3714–3725

Relating Structural and Thermodynamic Effects of the Pb(II) Lone Pair: A New Picolinate Ligand Designed to Accommodate the Pb(II) Lone Pair Leads to High Stability and Selectivity

Aymeric Pellissier, Yann Bretonnière, Nicholas Chatterton, Jacques Pécaut, Pascale Delangle, and Marinella Mazzanti*

Laboratoire de Reconnaissance Ionique et Chimie de Coordination, Service de Chimie Inorganique et Biologique (UMR-E 3 CEA-UJF), Département de Recherche Fondamentale sur la Matière Condensée, CEA-Grenoble, 38054 Grenoble, Cedex 09, France

Received September 25, 2006

The crystal and molecular structure and the stability of lead and calcium complexes of two chelates containing picolinate chelating groups in different geometries have been investigated in order to relate the ligand affinity and selectivity for lead over calcium with the ability of the ligand to accommodate a stereochemically active lone pair. The crystal structures of the lead complexes of the diprotonated and monoprotonated tripodal ligand $tpaa^{2-}$ show that the three picolinate arms of the tripodal ligand coordinate the lead in an asymmetric way leaving a gap in the coordination sphere to accommodate the lead lone pair. As a consequence of this binding mode, one picolinate arm is very weakly bound and therefore can be expected to contribute very little to the complex stability. Conversely, the geometry of the dipodal ligand H_2dpaea is designed to accommodate the lead lone pair; in the structure of the [Pb(dpaea)] complex the donor atoms of the ligand occupy only a quarter of the coordination sphere, reducing the sterical interaction between the lead lone pair with respect to the H_3tpaa complexes. As a result, in the lead structures of H_2dpaea all the ligand donor atoms are strongly bound to the metal ion leading to increased stability. The high value of the formation constant measured for the lead complex of the dipodal $dpaea^{2-}$ ($\log \beta_{11}(Pb) = 12.1(3)$) compared to the lower value found for the one of the tripodal $tpaa^{3-}$ ($\log \beta_{11}(Pb) = 10.0(1)$) provides direct evidence of the influence of the stereochemically active lead lone pair on complex stability. As a result, since the ligand geometry has little effect on the stability of the calcium complex, a remarkable increase in the Pb/Ca selectivity is observed for $dpaea^{-}$($10^{6.6}$) compared to $tpaa^{3-}$ ($10^{1.5}$), making the dipodal ligand a good candidate for application as extracting agent for the lead removal from contaminated water.

Introduction

There has recently been a resurgence of interest in the fascinating coordination chemistry of divalent lead motivated by the toxicity of lead and its widespread occurrence in the environment as a result of its numerous industrial applications. Indeed, a good knowledge of the coordination properties leading to preferential binding of lead over other essential metal ions is crucial for the understanding of the toxicological properties of lead, the design of selective chelation therapy agents, and the development of efficient chelating agents for the remediation of polluted water and soil.[1−3] Several recent studies focused on the design of chelating ligands for the removal of lead from contaminated water[4] and soils[5−8] by solvent extraction or liquid/solid extraction. The most

* To whom correspondence should be addressed. E-mail: marinella.mazzanti@cea.fr.

(1) Claudio, E. S.; Godwin, H. A.; Magyar, J. S. *Prog. Inorg. Chem.* **2003**; Vol. 51, pp 1−144.
(2) Farrer, B. T.; Pecoraro, V. L. *Curr. Opin. Drug Discov. Dev.* **2002**, *5*, 937−943.
(3) Magyar, J. S.; Weng, T. C.; Stern, C. M.; Dye, D. F.; Rous, B. W.; Payne, J. C.; Bridgewater, B. M.; Mijovilovich, A.; Parkin, G.; Zaleski, J. M.; Penner-Hahn, J. E.; Godwin, H. A. *J. Am. Chem. Soc.* **2005**, *127*, 9495−9505.
(4) Cuenot, F.; Meyer, M.; Bucaille, A.; Guilard, R. *J. Mol. Liq.* **2005**, *118*, 89−99.
(5) Rampley, C.; Ogden, K. L. *Environ. Sci. Technol.* **1998**, *32*, 987−993.
(6) Tandy, S.; Bossart, K.; Mueller, R.; Ritschel, J.; Hauser, L.; Schulin, R.; Nowack, B. *Environ. Sci. Technol.* **2004**, *38*, 937−944.
(7) Kim, C.; Lee, Y.; Ong, S. K. *Chemosphere* **2003**, *51*, 845−853.
(8) Grcman, H.; Vodnik, D.; Velikonja-Bolta, S.; Lestan, D. *J. Environ. Qual.* **2003**, *32*, 500−506.

10.1021/ic061823d CCC: $37.00
Published on Web 04/06/2007

common chelator studied in the literature is EDTA which has been used to remove lead nitrate from wastewater. Despite this, EDTA strongly chelates a large variety of ions, limiting the possibility of its application in the removal of lead from contaminated water or soils. The feasibility of lead contamination remediation by chelation requires a high selectivity of the chelating agent for Pb(II) relative to Ca(II) and other alkaline or earth-alkaline ions due to the usually higher concentration of these ions in polluted water or some soils. Soft donor ligands have better affinity for Pb(II) than for Ca(II) as predicted by the Pearson's hard−soft rule,[9] and on this basis a lead-selective sequestering agent has been developed by grafting a tetraacetamide cyclam derivative on silica surface.[10] However, in the design of selective multidentate ligands, besides the nature of donor atoms other parameters such as coordination geometry, sterical effects, or chelate ring size can play an important role. Divalent lead shows unusual and very rich coordination chemistry with a wide variety of coordination numbers and irregular geometries. The donor atoms can distribute spherically around the lead(II) ion in what have been defined as "holodirected" structures where the lead lone pair is stereochemically inactive, or they can cluster to one side leaving an "open" coordination site to accommodate the stereochemically active 6s lone pair ("hemidirected structures"). Several studies have been directed in the past few years to rationalize the structural effects of the lead lone pair.[11−19] Reger and co-workers have shown that the stereoactivity of the lead lone pair can be controlled by varying the substituents on tris(pyrazolyl)borate ligands.[20−23] However, few systematic studies have been reported in which both the structure and the stability of lead complexes have been investigated,[16,24−27] making it difficult to relate the ligand affinity and selectivity for lead with a preferred coordination geometry or with the presence of a stereochemically active lone pair.

Chart 1

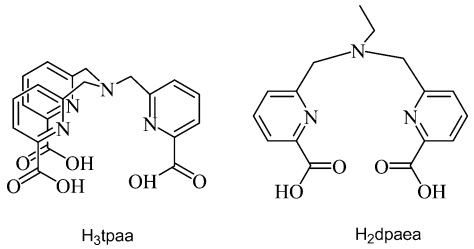

Hancock and Martell on the basis of their study of a series of macrocyclic complexes suggested that increasing the number of nitrogen atoms in the ligand increases the affinity for lead by the activation of the stereochemical lone pair.[27,28] Nevertheless, in spite of the fact that all the lead complexes of ligands currently used as chelation therapy agents to treat lead poisoning have stereochemically active lone pairs, at this point it remain unclear if ligands with geometry that can accommodate a stereochemically active lone pair yield a higher affinity for lead and an improved selectivity for lead over other metal ions. In this paper, we report the molecular structures and the formation constants of the calcium and lead complexes of the heptadentate trispicolinate ligand tpaa (H_3tpaa = α,α′,α″-nitrilotri(6-methyl-2-pyridinecarboxylic acid) and of the new pentadentate bispicolinate ligand dpaea^{2-} (H_2dpaea = *N*,*N*-bis[(6-carboxypyridin-2-yl)-methyl]ethylamine), Chart 1. A previous study of the coordination chemistry of the tpaa^{3-} ligand shows that it binds strongly in a heptadentate fashion to lanthanide(III) ions and divalent calcium.[29] In the present work, we find that tpaa^{3-} binds lead preferentially with respect to calcium, probably due to the presence of soft pyridyl donors. In the design of the new ligand dpaea^{2-}, one picolinate arm is removed with respect to tpaa to better accommodate the lead lone pair resulting in an important increase of the affinity and selectivity for lead.

Experimental Section

General Information. ^{1}H NMR spectra were recorded on Bruker 200 and Varian U-400 spectrometers using D_2O solutions with D_2O and 3-(trimethylsilyl)-1-propansulfonic acid as internal standards. Mass spectra were measured with a Finnigan LC-Q instrument. Elemental analyses were performed by SCA/CNRS, Vernaison, France.

Solvents and starting materials were obtained from Aldrich, Fluka, Acros, and Alfa and used without further purification. 6-Chloromethylpyridine-2-carboxylic acid ethyl ester was obtained from the commercially available 2,6-dipicolinic acid according to a published procedure.[30] The ligand H_3tpaa, α, α′, α″-nitrilotri(6-

(9) Pearson, R. G. *J. Am. Chem. Soc.* **1963**, *85*, 3533.
(10) Cuenot, F.; Meyer, M.; Espinosa, E.; Guilard, R. *Inorg. Chem.* **2005**, *44*, 7895−7910.
(11) Bashall, A.; McPartlin, M.; Murphy, B. P.; Fenton, D. E.; Kitchen, S. J.; Tasker, P. A. *J. Chem. Soc., Dalton Trans.* **1990**, 505−509.
(12) Bashall, A.; McPartlin, M.; Murphy, B. P.; Powell, H. R.; Waikar, S. *J. Chem. Soc., Dalton Trans.* **1994**, 1383−1390.
(13) Parr, J. *Polyhedron* **1997**, *16*, 551−566.
(14) Shimoni-Livny, L.; Glusker, J. P.; Bock, C. W. *Inorg. Chem.* **1998**, *37*, 1853−1867.
(15) Hancock, R. D.; Reibenspies, J. H.; Maumela, H. *Inorg. Chem.* **2004**, *43*, 2981−2987.
(16) Luckay, R.; Cukrowski, I.; Mashishi, J.; Reibenspies, J. H.; Bond, A. H.; Rogers, R. D.; Hancock, R. D. *J. Chem. Soc., Dalton Trans.* **1997**, 901−908.
(17) Arnaud-Neu, F.; Harrowfield, J. M.; Michel, S.; Skelton, B. W.; White, A. H. *Supramol. Chem.* **2005**, *17*, 609−615.
(18) Esteban-Gomez, D.; Ferreiros, R.; Fernandez-Martinez, S.; Avecilla, F.; Platas-Iglesias, C.; de Blas, A.; Rodriguez-Blas, T. *Inorg. Chem.* **2005**, *44*, 5428−5436.
(19) Pedrido, R.; Bermejo, M. R.; Romero, M. J.; Vazquez, M.; Gonzalez-Noya, A. M.; Maneiro, M.; Rodriguez, M. J.; Fernandez, M. I. *Dalton Trans.* **2005**, 572−579.
(20) Reger, D. L.; Huff, M. F.; Rheingold, A. L.; Haggerty, B. S. *J. Am. Chem. Soc.* **1992**, *114*, 579−584.
(21) Reger, D. L.; Collins, J. E.; Rheingold, A. L.; Liable-Sands, L. M.; Yap, G. P. A. *Inorg. Chem.* **1997**, *36*, 345−351.
(22) Reger, D. L.; Wright, T. D.; Little, C. A.; Lamba, J. J. S.; Smith, M. D. *Inorg. Chem.* **2001**, *40*, 3810−3814.
(23) Reger, D. L.; Little, C. A.; Smith, M. D.; Rheingold, A. L.; Liable-Sands, L. M.; Yap, G. P. A.; Guzei, I. A. *Inorg. Chem.* **2002**, *41*, 19−27.
(24) Clapp, L. A.; Siddons, C. J.; VanDerveer, D. G.; Reibenspies, J. H.; Jones, S. B.; Hancock, R. D. *Dalton Trans.* **2006**, 2001−2007.
(25) Bridgewater, B. M.; Parkin, G. *J. Am. Chem. Soc.* **2000**, *122*, 7140−7141.
(26) Rupprecht, S.; Langemann, K.; Lugger, T.; McCormick, J. M.; Raymond, K. N. *Inorg. Chim. Acta* **1996**, *243*, 79−90.
(27) Hancock, R. D.; Shaikjee, M. S.; Dobson, S. M.; Boeyens, J. C. A. *Inorg. Chim. Acta* **1988**, *154*, 229−238.
(28) Hancock, R. D.; Martell, A. E. *Chem. Rev.* **1989**, *89*, 1875−1914.
(29) Bretonnière, Y.; Mazzanti, M.; Dunand, F. A.; Merbach, A. E.; Pécaut, J. *Chem. Commun.* **2001**, 621.

methyl-2-pyridinecarboxylic acid, was prepared from 2,6-dipicolinic acid according to the previously reported procedure.[29,31]

***N,N*-Bis[(6-carbethoxypyridin-2-yl)methyl]ethylamine.** A solution of anhydrous K_2CO_3 (5.53 g, 40.0 mmol) in anhydrous acetonitrile (50 mL) and a solution of 6-chloromethylpyridine-2-carboxylic acid ethyl ester (5.23 g, 26.2 mmol) in anhydrous acetonitrile (30 mL) were successively added under argon atmosphere to 0.98 g (12.1 mol) $EtNH_2$_HCl. The reaction mixture was refluxed for 4 days. After filtration and evaporation of the solvent, a yellow oil was obtained which was dissolved in dichloromethane (100 mL). The resulting solution was washed twice with a 1 M water solution of $NaHCO_3$ (50 mL) and then dried over anhydrous Na_2SO_4. After evaporation of the solvent, the resulting brown solid (3.6 g, 9.7 mmol, 79% yield) was used without further purification.

RMN ^{1}H (CD_3CN, 200 MHz): δ 1.12 (3H, t, J = 7.0 Hz, CH_2CH_3); 1.40 (6H, t, J = 7.0 Hz, $COOCH_2CH_3$); 2.63 (2H, q, J = 7.0 Hz, CH_2CH_3); 3.86 (4H, s, H_4); 4.40 (4H, q, J = 7.0 Hz, $COOCH_2CH_3$); 7.81 (2H, d, J = 7.7 Hz, H_3); 7.86 (2H, t, J = 7.7 Hz, H_2); 7.93 (2H, d, J = 7.7 Hz, H_1).

ES-MS (m/z): 372.1 $[M + H]^+$; 394.2 $[M + Na]^+$.

***N,N*-Bis[(6-carboxypyridin-2-yl)methyl]ethylamine (H_2dpaea).** Bis[(6-carbethoxypyridin-2-yl)methyl-ethylamine (3.6 g, 9.7 mmol) was dissolved in ethanol (200 mL). A 1 M solution of potassium hydroxide in water (35 mL) was added, and the mixture was refluxed for 20 h. The solvent was then evaporated under reduced pressure, and the resulting solid was dissolved in water (10 mL). The solution was acidified with concentrated HCl to pH 7, and a white precipitate was filtered off. The solution was further acidified (to pH $\sim$ 2) and refrigerated (0 °C) overnight. An off-white solid formed. A second crop of solid was obtained by evaporation of the resulting solution and recrystallization from methanol to yield 1.09 g (3.1 mmol, 32%) of the desired ligand.

RMN ^{1}H (D_2O, 200 MHz, pD = 2) : δ 1.49 (3H, t, J = 7.0 Hz, CH_2CH_3); 3.59 (2H, q, J = 7.0 Hz, CH_2CH_3); 4.67 (4H, s, H_4); 7.52 (2H, d, J = 7.7 Hz, H_3); 7.87 (4H, m, H_1, H_2).

ES-MS (m/z) : 316.3 $[M + H]^+$; 272.1 $[M - CO_2 + H]^+$; 179.1 $[M - CO_2 - C_4H_4NCH_3 + H]^+$; 135.2 $[M - 2CO_2 - C_4H_4NCH_3 + H]^+$.

Anal.Calcd for H_2dpaea_HCl_1.5KCl, $C_{16}H_{17}N_3O_4Cl$: C 41.34, H 3.96, N 9.02. Found: C, 41.45, H 3.91, N 9.06.

Crystals of the lead complexes of $dpaea^{2-}$ and of $Hdpaea^-$ were isolated by slow evaporation of 10^{-2} M solutions of H_2-dpaea_HCl_1.5KCl and $PbCl_2$ in 1:1 ratio after adjusting the pH with a 0.1 M KOH water solution, respectively, to 3.6 and 1.5.

Crystals of the lead complexes of $Htpaa^{2-}$ and of H_2tpaa^- were isolated by slow evaporation of 10^{-2} M solutions of H_3tpaa and $PbCl_2$ in 1:1 ratio after adjusting the pH with a 0.1 M KOH water solution, respectively, to 5.6 and 1.6.

Crystals of the calcium complex of $dpaea^{2-}$ were obtained by slow diffusion of a 1 M methanol solution of KOH into a methanol solution of H_2dpaea_HCl_1.5KCl and $CaCl_2$ in 1:1 ratio.

Crystals of the calcium complex of $tpaa^{3-}$ were obtained by slow evaporation of a 10^{-3} M water solution of H_3tpaa and $CaCl_2$ in 1:1 ratio after adjusting the pH at 7.0.

10^{-2} M D_2O solutions of the lead complexes of H_3tpaa and H_2-dpaea for NMR studies were prepared in situ.

X-ray Crystallography. All the crystals were analyzed using a Bruker SMART CCD area detector three-circle diffractometer (Mo Kα radiation, graphite monochromator, λ = 0.71073 Å). The cell parameters were obtained with intensities detected on three batches of 15 frames with a 5 s exposure time for complexes **1**−**2** and a 10 s exposure for compounds **3**−**7**. The crystal−detector distance was 5 cm. For three settings of Φ narrow data frames were collected for 0.3° increments in ω. A hemisphere of data was collected for compounds **1**−**3** and **5**−**7** (a quadrant was collected for complex **4**). At the end of data collection, the first 50 frames were re-collected to establish that crystal decay had not taken place during the collection. Unique intensities with $I > 10\sigma(I)$ detected on all frames using the Bruker program[32] were used to refine the values of the cell parameters. The substantial redundancy in data allows empirical absorption corrections to be applied using multiple measurements of equivalent reflection with the SADABS Bruker program.[32] Space groups were determined from systematic absences, and they were confirmed by the successful solution of the structure (see Table 1). Complete information on crystal data and data collection parameters is given in the Supporting Information.

The structures were solved by direct methods using the SHELX-TL 6.14 package[33] and, for all structures, except for complex **2,** all atoms, including hydrogen atoms, were found by difference Fourier syntheses. All non-hydrogen atoms were anisotropically refined on F^2. Hydrogen atoms were refined isotropically. For complex **2**, hydrogen atoms were included in calculated positions and refined isotropically.

Potentiometric Titrations. All solutions were prepared using water purified by passing through a Millipore Milli-Q reverse-osmosis cartridge system (resistivity 18 MΩ cm). Carbonate-free 0.1 M KOH and 0.1 M HCl were prepared from Fisher Chemicals concentrates. Ligand concentration was determined by alkalimetric titration. Metal solutions were prepared by dissolving the appropriate amount of $PbCl_2$ or $CaCl_2$ in water. The exact metal ion concentration was determined by colorimetric titration using standardized EDTA solutions (Fisher Chemicals) and xylenol orange or calcon as indicator, respectively, for Pb^{2+} or Ca^{2+}.

Potentiometric titrations were performed in a thermostated cell (25 ± 0.1 °C) under an argon atmosphere, and the ionic strength was fixed with KCl 0.1 M. The p[H] (p[H] = $-\log[H^+]$, concentration in molarity) was measured in each titration with a combined pH glass electrode (Metrohm) filled with 3 M KCl, and the titrant addition was automated by use of a 751 GPD titrino (Metrohm). The electrode was calibrated in hydrogen ion concentration by titration of a known amount of HCl by 0.1 M KOH in 0.1 M KCl. A plot of meter reading versus p[H] allows the determination of the electrode standard potential ($E°$) and the slope factor (f).[34] Solutions (20 mL) of H_3dpaea^+ (0.001 or 0.0005 M) or H_3tpaa (0.0005 M) alone or of 1:1 metal/ligand mixtures were titrated with a 0.1 M KOH solution. Back-titration with 0.1 mol L^{-1} HCl were systematically performed after each experiment to check whether equilibration had been achieved. There were 100 points measured with 5 min waiting between 2 points.

Experimental data were refined using the computer program Hyperquad 2000.[35,36] All equilibrium constants are concentration quotients rather than activities. The ionic product of water at 298 K and 0.1 M ionic strength is pK_w = 13.78.[37] All values and errors (one standard deviation) reported represent the average of at least 3 independent experiments.

(30) Fornasier, R.; Milani, D.; Scrimin, P.; Tonellato, U. *J. Chem. Soc., Perkin Trans. 2* **1986**, 233−237.
(31) Bretonnière, Y.; Mazzanti, M.; Dunand, F. A.; Merbach, A. E.; Pécaut, J. *Inorg. Chem.* **2001**, *40*, 6737−6745.
(32) *SADABS*; Bruker: Madison, WI, 1995.
(33) Sheldrick, G. M. *SHELXTL 6.14*, 5 ed.; University of Göttingen: Göttingen, Germany, 1994.
(34) Martell, A. E.; Motekaitis, R. J. *Determination and use of stability constants*; VCH: New York, 1992.
(35) Alderighi, L.; Gans, P.; Ienco, A.; Peters, D.; Sabatini, A.; Vacca, A. *Coord. Chem. Rev.* **1999**, *184*, 311−318.
(36) Gans, P.; Sabatini, A.; Vacca, A. *Talanta* **1996**, *43*, 1739−1753.

Table 1. Crystallographic Data for the Structure of H_2dpaea and the Six Structures of Complexes **2**–**7**

	H_2dpaea_2H_2O, **1**	[Pb(H_2tpaa)Cl]_2H_2O, **2**	[Pb(Htpaa)]$_2$_4H_2O, **3**	[Pb(Hdpaea)Cl, **4**	[Pb(dpaea)].[Pb(dpaea)H_2O)]_6H_2 O, **5**	[Ca(dpaea)(H_2O)-(M eOH)]$_2$, **6**	{[Ca(tpaa)(H_2O)]$_2$ Ca(H_2O)$_4$}, **7**
formula	$C_{16}H_{21}N_3O_6$	$C_{21}H_{17}ClN_4O_6Pb$	$C_{21}H_{20}N_4O_8Pb$	$C_{16}H_{16}ClN_3O_4Pb$	$C_{32}H_{44}N_6O_{15}Pb_2$	$C_{34}H_{42}Ca_2N_6O_{12}$	$C_{42}H_{58}Ca_3N_8O_{26}$
fw	351.36	664.03	663.60	556.96	1167.11	806.90	1211.20
T, K	298(2)	298(2)	123(2)	298(2)	193(2)	298(2)	193(2)
cryst syst	triclinic	triclinic	triclinic	orthorhombic	triclinic	monoclinic	monoclinic
space group	$P\bar{1}$	$P\bar{1}$	$P1$	*Pnma*	$P1$	$P2_1/n$	$C2/c$
a, Å	9.8539(13)	7.7921(6)	8.8430(7)	15.42(2)	10.3489(7)	12.095(2)	30.823(4)
b, Å	12.7185(16)	11.3321(9)	9.4690(7)	16.421(19)	11.4285(7)	12.964(2)	9.1597(14)
c, Å	14.0516(17)	13.8880(11)	14.0962(11)	6.781(13)	16.6686(11)	12.273(2)	21.278(3)
α, deg	100.489(2)	66.8760(10)	89.8610(10)	90	90.7770(10)	90	90
β, deg	95.553(2)	82.5020(10)	88.1640(10)	90	103.9400(10)	94.247(3)	116.377(3)
γ, deg	93.837(3)	73.0390(10).	62.5240(10)	90	95.4220(10)	90	90
V, Å^3, Z	1717.0(4), 4	1078.6(1), 2	1046.6(1), 2	1717(5), 4	1903.5(2), 2	1919.1(6), 2	5381.9(1), 4
D_{calcd}, g cm^{-3}	1.359	2.045	2.106	2.154	2.036	1.396	1.495
μ (Mo Kα), mm^{-1}	0.105	7.993	8.120	10.006	8.910	0.365	0.401
R1, wR2,[a] [$I > 2\sigma(I)$]	0.0683, 0.2141	0.0376, 0.0879	0.0295, 0.0760	0.0418, 0.1131	0.0460, 0.1276	0.0492, 0.1106	0.0564, 0.1304

[a] Structure was refined on F_o^2 using all data: wR2 = $[\Sigma[w(F_o^2 - F_c^2)^2]/\Sigma[w(F_o^2)^2]]^{1/2}$, where $w^{-1} = [\Sigma(F_o^2) + (aP)^2 + bP]$ and $P = [\max(F_o^2, 0) + 2F_c^2]/3$.

Figure 1. ORTEP diagram of the diprotonated ligand H_2dpaea (**1**) with thermal ellipsoids at 30% probability.

Scheme 1

Results and Discussion

Synthesis and Structure of the Ligand H_2dpaea. *N*,*N*-Bis[(6-carboxypyridin-2-yl)methyl]ethylamine (H_2dpaea) was obtained in 2 steps using the synthetic route detailed in Scheme 1 with a global yield of 25% from the previously described 6-chloromethylpyridine-2-carboxylic acid ethyl ester. The desired ligand was isolated in its triprotonated cationic form from a water solution after adjusting the pH to 2. The proton NMR spectra show all the expected resonances, and satisfactory elemental analytical data were obtained. The proton NMR spectra recorded at different pH show a significant shift (0.5 ppm) of the methylene protons between pH =7 and pH = 10 due to the protonation of the aliphatic nitrogen. Crystals of the neutral diprotonated ligand H_2dpaea (**1**) were obtained by slow evaporation of a water solution of **1** at pH = 7.

The structure of **1** is shown in Figure 1. Two molecules of H_2dpaea are linked by two strong hydrogen bonds between a carboxylate oxygen from each molecule and a carboxylic hydrogen from the other molecule (O(2)···O(11), 2.512(2) Å; (O(2)−H(2O)···O(11), 175(3)°) leading to the formation of a centrosymmetric dimer. The ligand adopts a zwitterionic form with one protonated carboxylate group, a deprotonated carboxylate group, and a protonated tertiary amine nitrogen.

(37) Smith, R. M.; Martell, A. E.; Motekaitis, R. J. *NIST Critically Selected Stability Constants of Metal Complexes Database*; NIST Standard Reference Database 46, 2001.

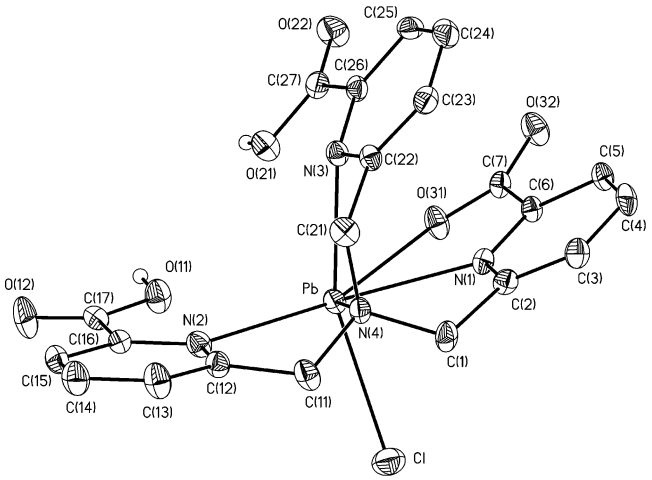

Figure 2. ORTEP diagram of the complex [Pb(H_2tpaa)Cl] (**2**) with thermal ellipsoids at 30% probability.

This leads to a dipodal conformation of the neutral pentadentate H_2dpaea preorganized for metal complexation. A similar preorganized zwitterionic structure was previously found for the neutral ligand H_3tpaa.

Crystal and Molecular Structure of Lead Complexes. The lead(II) ion has a lone pair of electrons which can be stereochemically active and can have important effects on the structure of its complexes.

In the structures of lead complexes where the lone pair has no steric effects (inactive lone pair or holodirected[14]), all the Pb−L bonds have similar lengths after taking into account the differences in ionic radii of the different donor atoms. It has been observed that Pb−N bond lengths fall for these complexes in the range 2.62−2.88 Å.[27] The steric effects which have been generally associated with the presence of an active lone pair are the following: (1) the presence of a gap in the coordination at the site of the lone pair or very long Pb−L bonds at this site, (2) a shortening of the Pb−L bond lengths for the ligands located in a site opposite to the position of the lone pair, and (3) a lengthening of those adjacent to this site.

In this context, we have determined and analyzed the structures of several complexes of lead with the Hdpaea$^-$, dpaea^{2-}, H_2tpaa$^-$, and tpaa^{2-} ligands in an attempt to rationalize the difference in the thermodynamic stability of these lead picolinate complexes in terms of their structural properties.

Slow evaporation of water solutions of the picolinate ligands (H_2dpaea or H_3tpaa) and $PbCl_2$ in 1:1 ratio lead to the isolation of different species depending on the pH.

The complex [Pb(H_2tpaa)Cl] (**2**) was isolated by slow evaporation of a water solution at pH = 1.6. The crystal structure of **2** is shown in Figure 2, and selected interatomic distances and angles are given in Table 2. The metal ion can be regarded as six-coordinated by four nitrogens and one oxygen of the monoanionic diprotonated H_2tpaa$^-$ acting as a pentadentate ligand and by a chloride with irregular coordination geometry. However, the two oxygen atoms of the protonated carboxylic groups are situated at distances (Pb−O(21) = 2.980(6) Å and Pb−O(11) = 3.028(6) Å) longer than the sum of the ionic radii, but shorter than the sum of the van der Waals radii.[38] Similar Pb−O distances have been previously interpreted in terms of coordinating oxygen atoms located close to the site occupied by the sterically active lead lone pair.[24] A similar interpretation for the structure of complex **2** would result in an eight-coordinated lead ion and would suggest the presence of an active lone pair in the proximity of the carboxylic oxygens. Although not obvious, the presence of an active lone pair could explain the highly asymmetric arrangement of the N-donors with Pb−N distances ranging from 2.646(6) to 2.803(6) Å. At longer distance (Pb−O(22) =3.374 Å) is found for the carbonyl oxygen of the one protonated carboxylic group.

Table 2. Selected Bond Lengths (Å) and Angles (deg) in the Complex [Pb(H_2tpaa)Cl] (**2**)

Pb−N(1)	2.645(6)
Pb−O(31)	2.654(5)
Pb−N(4)	2.658(6)
Pb−N(3)	2.720(6)
Pb−Cl	2.763(2)
Pb−N(2)	2.803(6)
N(1)−Pb−O(31)	59.90(18)
N(1)−Pb−N(4)	63.81(19)
O(31)−Pb−N(4)	121.99(17)
N(1)−Pb−N(3	67.73(19)
O(31)−Pb−N(3)	80.78(18)
N(4)−Pb−N(3)	65.99(19)
N(1)−Pb−Cl	86.10(15)
O(31)−Pb−Cl	106.17(15)
N(4)−Pb−Cl	82.37(15)
N(3)−Pb−Cl	145.26(14)

The pseudo-C_3 symmetry observed in the crystal structure of the free triprotonated ligand and in its lutetium(III) complex[31] is disrupted by the inversion of the orientation of one picolinate arm.

While the high water solubility of the anionic lead complex [Pb(tpaa)]$^-$ prevented the isolation of crystals of this species in the pH range 5−10, crystals of the neutral complex [Pb(Htpaa)]$_2$ (**3**) were obtained from slow evaporation of water solutions at pH = 5.6. The structure of **3** is shown in Figure 3, and selected bond distances and angles are given in Table 3. The lead complex of the monoprotonated tpaa crystallizes as a centrosymmetric dimer through the formation of strong hydrogen bonds between the protonated carboxylic group (O(12)) and one carboxylate oxygen (O(2)). A similar dimeric structure had been found for the free ligand.[31] The ligand coordinates to the metal leaving a large gap in the coordination geometry, most likely the site of an active lone pair. The lead ion appears to be pentacoordinated by the two bidentate picolinate arms and by the apical nitrogen of the tripodal ligand with irregular coordination geometry. In this description, the third bidentate picolinate is regarded as nonchelating due to the rather long Pb−O (3.329(3) Å) and Pb−N(2) (3.011(4) Å) distances. These values are, however, shorter than the sum of the van der Waals radii,[38] and the picolinate arm is located in proximity of the active lone pair. The value of the Pb−N(1) distance is short (2.509(4) Å), as

(38) Bondi, A. *J. Phys. Chem.* **1964**, *68*, 441.

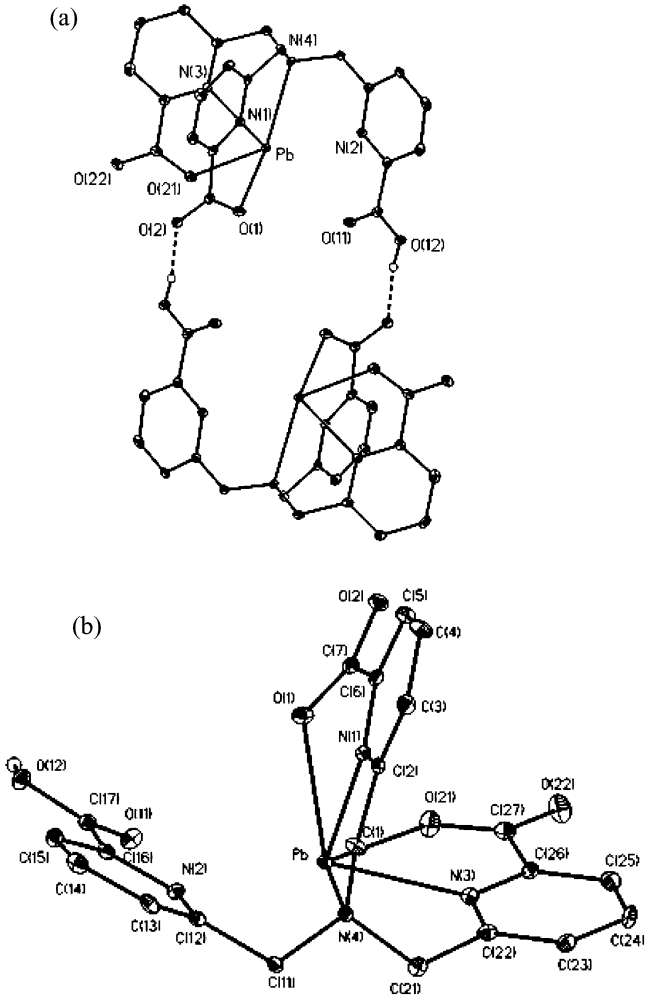

Figure 3. Side view of the molecular structure of the dimeric complex $[Pb(Htpaa)]_2$ (**3**) and (a) top view of the asymmetric unit (b) with thermal ellipsoids at 30% probability.

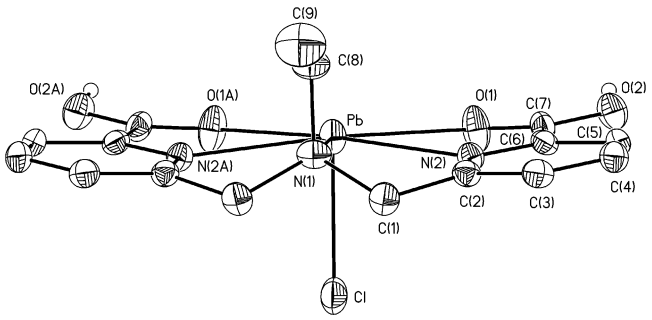

Figure 4. ORTEP diagram of the complex $[Pb(Hdpaea)Cl]_2$ (**4**) with thermal ellipsoids at 30% probability.

expected for Pb−L bonds located opposite to the site of the active lone pair confirming its presence, while the Pb−L bonds become increasingly longer when approaching the site of the lone pair (L = N(4) and O(1)). In an alternative interpretation of the coordination geometry, the third picolinate arm could be regarded as weakly coordinating because it is lying adjacent to the active lone pair. In the crystal structure of the analogous neutral lead complex [Pb(Hsaltren)] of the potentially heptadentate tripodal Schiff basis H_3saltren [(*N*-salicylideneamino)ethyl] previously described by Parr and co-workers,[39] one of the ligand arms is bent away and only two nitrogen and two oxygen atoms of the ligand are unambiguously coordinated to the metal ion.

Table 3. Selected Bond Lengths (Å) and Angles (deg) in the Complex [Pb(Htpaa)] (**3**)

Pb−(1)	2.509(4)
Pb−O(1)	2.599(3)
Pb−O(21)	2.482(4)
Pb−N(4)	2.728(4)
Pb−N(3)	2.540(4)
Pb−N(2)	3.011(4)
Pb−O(11)	3.329(3)
N(1)−Pb−O(21)	94.45(13)
N(4)−Pb−O(21)	128.76(11)
N(3)−Pb−O(21)	64.56(12)
O(1)−Pb−O(21)	69.36(12)
N(1)−Pb−N(4)	65.70(11)
O(1)−Pb−N(4)	127.93(11)
N(1)−Pb−N(3)	76.36(12)
O(1)−Pb−N(3)	115.21(12)
N(4)−Pb−N(3)	64.94(12)
O(1)−Pb−N(1)	64.40(11)
O(21)−Pb−N(2)	168.50(11)
N(1)−Pb−N(2)	88.19(11)
N(3)−Pb−N(2)	126.90(11)
O(1)−Pb−N(2)	102.00(11)
N(4)−Pb−N(2)	62.40(11)
O(21)−Pb−O(11)	118.56(10)
N(1)−Pb−O(11)	108.30(10)
N(3)−Pb−O(11)	173.62(10)
O(1)−Pb−O(11)	71.07(10)
N(4)−Pb−O(11)	112.57(10)
N(2)−Pb−O(11)	50.17(9)

Both structures of the isolated lead complexes **2** and **3** of the H_3tpaa ligands suggest that only two picolinate arms contribute significantly to the lead binding in the isolated species due to the proximity of the third bidentate picolinate arm to the site of the lead lone pair. These observations incited us to design a new ligand presenting only two picolinate arms which could occupy the quarter of sphere opposite to the active site. Such geometry regrouping all the donor atoms away from the site of the lone pair is expected to give rise to an increased affinity for the lead(II) ion,[16] and therefore, the study of the structure and thermodynamic stability of the lead complexes of H_2dpaea should allow us to shed light on the proposed relation between the presence of an active lead lone pair and the affinity for lead.

In order to confirm the expected arrangement of the coordinating atoms in the lead complexes of the bis-picolinate ligand, the crystal structures of two complexes isolated at different pH were determined. The complex [Pb(Hdpaea)Cl] (**4**) was isolated from a water solution at pH = 1.6. The structure of **4** is shown in Figure 4, and selected bond distances and angles are given in Table 4. The crystal structure of **4** shows that strong hydrogen bonds between the protonated carboxylic acid and the oxygen carboxylate

(39) Parr, J.; Ross, A. T.; Slawin, A. M. Z. *J. Chem. Soc., Dalton Trans.* **1996**, 1509−1512.

Table 4. Selected Bond Lengths (Å) and Angles (deg) in the Complex [Pb(Hdpaea)Cl] (**4**)[a]

Pb−Cl	2.5941(15)
Pb−O(1)	2.684(3)
Pb−N(2)	2.607(3)
Pb−N(1)	2.639(5)
Cl−Pb−N(2)	84.45(5)
Cl−Pb−N(1)	87.79(7)
N(2)−Pb−N(1)	65.37(6)
Cl−Pb−O(1)	90.35(5)
N(2)−Pb−O(1)	61.85(11)
N(1)−Pb−O(1)	127.11(7)
N(2)−Pb−O(1)#	166.40(7)
N(2)−Pb−N(2)#	129.76(13)
O(1)−Pb−O(1)	105.75(13)

[a] Symmetry transformations used to generate equivalent atoms: # indicates $x, -y + {}^1/_2, z$.

link the individual Pb(II) molecular units into a monodimensional chain along the *b*-axis of the unit cell (Figure 5). The molecule [Pb(Hdpaea)Cl] (**4**) has a crystallographic symmetry plane passing through the Pb ion, the Cl, N(1), and C(9). The complex presents a pentacoordinated lead with a hemidirected pentagonal pyramidal geometry with the monoanionic monodeprotonated $Hdpaea^-$ acting as a pentadentate ligand. The pentagonal plane is formed by the N(1), N(2), N(2#), O(1), and O(1#) atoms with a mean deviation of 0.08°. The apical position is occupied by a coordinated chloride anion. The evident gap in the disposition of the ligands around the lead ion indicates the presence of a stereochemically active lone pair. There are no atoms located near (at distances shorter than 4 Å) the site of the lone pair. In complex **4**, the Pb−Cl bond is located opposite to the coordination void, and the value of the Pb−Cl distance (2.594(1) Å) is significantly shorter than the mean distances found in holodirected structures (2.88(8) Å)[14] and shorter than the value expected from the sum of the ionic radii (2.89 Å). The Pb−N distances (2.607(3) and 2.639(5) Å) are longer than the range of values indicated for hemidirected lead complexes (2.37−2.56 Å)[27,40] with coordination number lower than eight, but similar values have been found in a pentacoordinate lead complex with a thiosemicarbazone ligand for which the presence of an active lone pair has been suggested.[19] Due to the presence of the coordinated chloride, the two picolinate arms spread over a hemisphere (angle between the planes Pb, N(1), N(2), O(1) and Pb, O(1#), N(2#), N(2) = 9.0°).

At pH = 3.6, crystals of the lead complex of the dianionic $dpaea^{2-}$ were isolated. The crystal structure of the isolated species $[Pb(1)(dpaea)(H_2O)]_2 \cdot [Pb(2)(dpaea)] \cdot 6H_2O$ (**5**) consists of two independent lead complexes $[Pb(1)(dpaea)(H_2O)]_2$, **5a**, and [Pb(2)(dpaea)], **5b**, with $dpaea^{2-}$ acting as a pentadentate ligand in both molecules and differing for the presence of a coordinated water molecule presenting a short Pb−O distance [Pb(1)−O(3) = 2.631(2) Å]. In the complex $[Pb(1)(dpaea)(H_2O)]_2$, two neutral $[Pb(1)(dpaea)(H_2O)]$ species are joined by strong hydrogen bonds between the water molecule (O(3)) and the bound carboxylate oxygen (O(1)) to form a centrosymmetric dimer. The ORTEP diagram of this dimer is shown in Figure 6 while selected bond distances and angles for **5a** and **5b** are presented in Table 5. Complex **5a** adopts a hemidirected structure suggesting the presence of an active lone pair. The coordinating atoms are located in a hemisphere with the angle between the Pb(1) N(1) O(3) plane and the plane Pb(1) N(2) O(1) N(1) = 172.6°. Short bond distances are found for Pb(1)−N(3) (2.594(1)Å) and Pb(1)−O(11) (2.491(1)Å) located opposite to the site of the lone pair. At longer Pb−O distance are found a water molecule (Pb(1)−O(53) = 2.935 Å) and the carboxylate oxygen from the adjacent complex (Pb(1)−O(11) = 2.819 Å), both located near to the site of the active lone pair. If these atoms are regarded as weakly coordinating, the structure of **5a** can be alternatively described as a dimer consisting of two eight coordinated $[Pb(1)(dpaea)(H_2O)_2]$ complexes connected by two bridging carboxylates and two strong hydrogen bonds.

The structure of **5b** is shown in Figure 7. The lead ion adopts a distorted square pyramidal geometry with the atoms O(21), O(31), N(21), N(23) occupying the square plane (mean dev = 0.11 Å) and N(22) in the apical position. All the ligand donor atoms occupy less than a quarter of a sphere around the lead ion with the angle between the Pb(2), N(21), N(22), O(21) and Pb(2), N(21), N(23), O(31) =79.1°. The ligand atoms coordinate the lead ion in an asymmetric way as expected in the presence of an active lone pair. The lone pair should be located opposite to the atoms showing the shortest Pb−L bond distances (Pb(2)−N(23) = 2.560(2) Å and Pb(2)−O(21) = 2.408(1) Å). In the proximity of the site of the active lone pair, two water oxygens (O(51)) and (O(56)) and one carboxylate oxygen (O(21)) from an adjacent Pb(2) complex are situated at distances (Pb(2)−O(51) = 2.856, Pb(2)−O(56) = 3.043, and Pb(2)−O(21) = 2.831 Å) longer than the sum of the ionic radii, but shorter than the sum of the van der Waals radii.[38] In an alternative interpretation, these atoms lying adjacent to the active lone pair could be regarded as weakly coordinating, and the structure of **5b** could be described as a centrosymmetric dimer consisting of two eight coordinated lead complexes connected by two bridging carboxylates.

These results show that the geometry of the dipodal ligand H_2dpaea allows in all the determined structures for a large coordination gap where the lead lone pair can be accommodated, significantly reducing the interactions between the ligand donor atoms and the lead electronic lone pair with respect to the H_3tpaa complexes.

Crystal and Molecular Structure of Calcium Complexes. The calcium complex of the ligand $dpaea^{2-}$ crystallizes in the centrosymmetric dinuclear structure $[Ca(dpaea)(MeOH)(H_2O)]_2$ (**6**) in which two neutral $[Ca(dpaea)(MeOH)(H_2O)]$ complexes are connected trough two bridging carboxylate oxygen atoms. The ORTEP diagram of complex **6** is shown in Figure 8, and selected bond distances and angles are given in Table 6. Each calcium ion is eight-coordinated by the three nitrogen and the two oxygen donors of the $dpaea^{2-}$ ligand, by one water oxygen, one methanol oxygen, and a bridging carboxylate oxygen with a dodecahedron geometry. The

(40) Harrowfield, J. M.; Miyamae, H.; Skelton, B. W.; Soudi, A. A.; White, A. H. *Aust. J. Chem.* **1996**, *49*, 1121−1125.

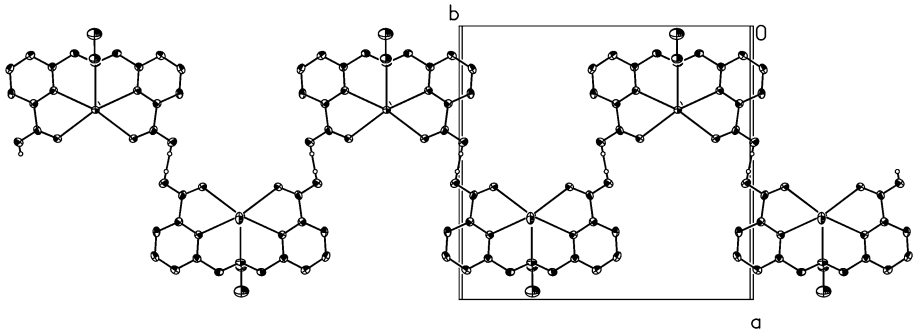

Figure 5. Top view of the H-bonded monodimensional chain of molecules of **4**.

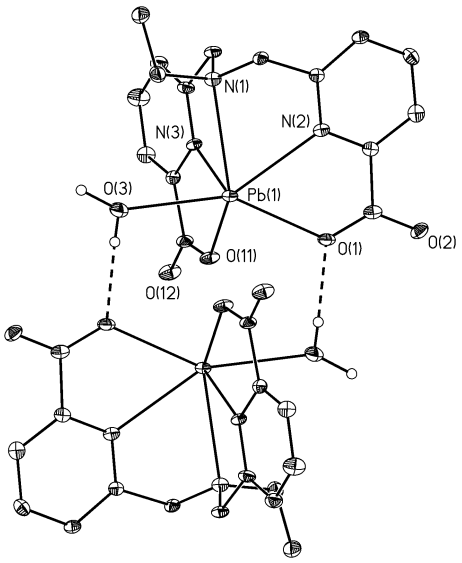

Figure 6. ORTEP diagram of the complex **5a** $[Pb(dpaea)(H_2O)]_2$ in **5** with thermal ellipsoids at 30% probability.

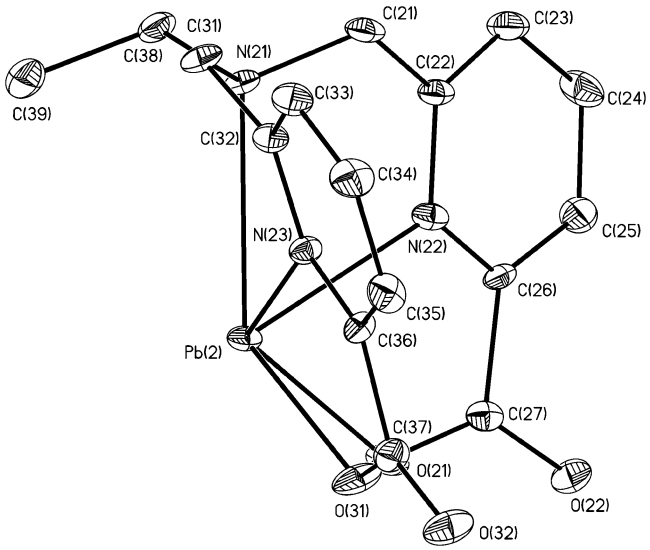

Figure 7. ORTEP diagram of the complex **5b** [Pb(dpaea)] in **5** with thermal ellipsoids at 30% probability.

Table 5. Selected Bond Lengths (Å) and Angles (deg) in the Complexes [Pb(1)(dpaea)(H_2O)] (**5a**) and [Pb(2)(dpaea)] (**5b**)

Pb(1)−O(11)	2.4907(14)	Pb(2)−O(31)	2.4082(14)
Pb(1)−N(3)	2.5941(15)	Pb(2)−O(21)	2.5256(17)
Pb(1)−O(1)	2.5958(16)	Pb(2)−N(23)	2.5601(16)
Pb(1)−O(3)	2.6308(19)	Pb(2)−N(22)	2.6215(18)
Pb(1)−N(2)	2.6543(18)	Pb(2)−N(21)	2.7951(16)
Pb(1)−N(1)	2.7842(15)		
O(11)−Pb(1)−N(3)	64.11(4)	O(31)−Pb(2)−O(21)	73.02(5)
O(11)−Pb(1)−O(1)	73.67(5)	O(31)−Pb(2)−N(23)	65.36(5)
N(3)−Pb(1)−O(1)	103.95(5)	O(21)−Pb(2)−N(23)	124.42(5)
O(11)−Pb(1)−O(3)	74.97(5)	O(31)−Pb(2)−N(22)	99.51(6)
N(3)−Pb(1)−O(3)	74.92(5)	O(21)−Pb(2)−N(22)	63.78(5)
O(1)−Pb(1)−O(3)	145.24(5)	N(23)−Pb(2)−N(22)	88.15(5)
O(11)−Pb(1)−N(2)	120.68(5)	O(31)−Pb(2)−N(21)	124.43(5)
N(3)−Pb(1)−N(2)	90.25(5)	O(21)−Pb(2)−N(21)	126.45(5)
O(1)−Pb(1)−N(2)	61.54(5)	N(23)−Pb(2)−N(21	61.84(5)
O(3)−Pb(1)−N(2)	151.41(5)	N(22)−Pb(2)−N(21)	63.46(5)
O(11)−Pb(1)−N(1)	127.27(5)		
N(3)−Pb(1)−N(1)	63.25(5)		
O(1)−Pb(1)−N(1)	122.36(5)		
O(3)−Pb(1)−N(1)	88.83(5)		
N(2)−Pb(1)−N(1)	62.60(5)		

mean Ca−N (2.66(16) Å) and Ca−O (2.44(7) Å) distances are similar to those found in other calcium polyaminocarboxylate complexes.[41]

The calcium complex of $tpaa^{3-}$ crystallizes in the centrosymmetric trinuclear structure $\{[Ca(1)(tpaa)(H_2O)]_2[Ca(2)(H_2O)_4]\}$ (**7**) in which two symmetric anionic $[Ca(1)(tpaa)(H_2O)]^-$ complexes are connected to the cationic aquo complex $[Ca(2)(H_2O)_4]^{2+}$ through two bridging O-donors derived from carboxylate groups and one bridging O-donor from a water molecule. The ORTEP diagram of complex **7** is shown in Figure 9, and selected bond distances and angles are given in Table 7.

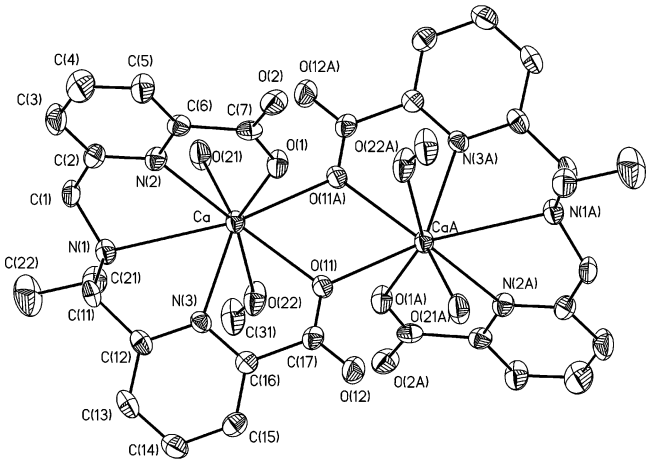

Figure 8. ORTEP diagram of the complex $[Ca(dpaea)(MeOH)(H_2O)]_2$ in **6** with thermal ellipsoids at 30% probability.

(41) Kumar, K.; Tweedle, M. F.; Malley, M. F.; Gougoutas, J. Z. *Inorg. Chem.* **1995**, *34*, 6472−6480.

Table 6. Selected Bond Lengths (Å) and Angles (deg) in the Complex $[Ca(dpaea)(H_2O)(MeOH)]_2$ (**6**)[a]

Ca−O(21)	2.349(3)		
Ca−O(1)	2.385(3)		
Ca−O(11)	2.458(2)		
Ca−O(22)	2.476(3)		
Ca−O(11)#	2.530(2)		
Ca−N(3)	2.543(3)		
Ca−N(2)	2.601(3)		
Ca−N(1)	2.846(3)		
Ca−Ca#	4.0624(14)		
O(21)−Ca−O(1)	110.86(11)	N(3)−Ca−N(2)	89.85(9)
O(21)−Ca−O(11)	145.29(11)	O(21)−Ca−N(1)	78.27(11)
O(1)−Ca−O(11)	75.84(8)	O(1)−Ca−N(1)	121.22(9)
O(21)−Ca−O(22)	86.07(11)	O(11)−Ca−N(1)	128.85(9)
O(1)−Ca−O(22)	146.92(10)	O(22)−Ca−N(1)	89.26(10)
O(11)−Ca−O(22)	74.65(9)	O(11)#−Ca−N(1)	155.04(9)
O(21)−Ca−O(11)#	77.98(10)	N(3)−Ca−N(1)	63.20(9)
O(1)−Ca−O(11)#	74.94(8)	N(2)−Ca−N(1)	60.27(9)
O(11)−Ca−O(11)#	70.93(10)	O(21)−Ca−Ca#	111.58(9)
O(22)−Ca−O(11)#	81.57(9)	O(1)−Ca−Ca#	71.95(6)
O(21)−Ca−N(3)	138.84(12)	O(11)−Ca−Ca#	36.05(6)
O(1)−Ca−N(3)	101.55(9)	O(22)−Ca−Ca#	75.44(7)
O(11)−Ca−N(3)	66.25(9)	O(11)#−Ca−Ca#	34.88(5)
O(22)−Ca−N(3)	79.81(10)	N(3)−Ca−Ca#	101.96(7)
O(11)#−Ca−N(3)	136.41(9)		
O(21)−Ca−N(2)	82.81(10)		
O(1)−Ca−N(2)	63.59(9)		
O(11)−Ca−N(2)	127.42(9)		
O(22)−Ca−N(2)	149.08(10)		
O(11)#−Ca−N(2)	123.63(9)		
N(2)−Ca−Ca#	135.44(8)		
N(1)−Ca−Ca#	160.75(7)		

[a] Symmetry transformations used to generate equivalent atoms: # indicates $-x + 2$, $-y$, $-z + 1$.

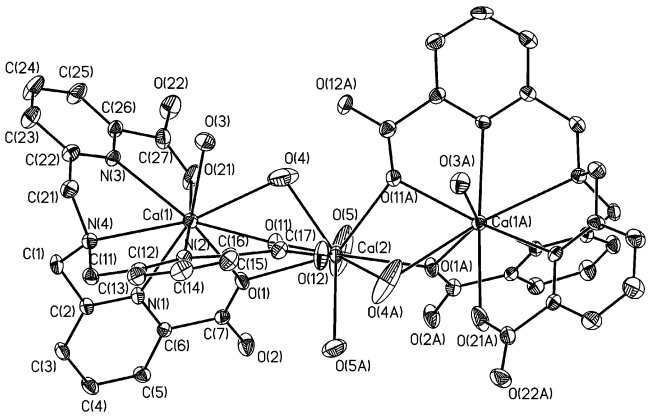

Figure 9. ORTEP diagram of the complex $\{[Ca(tpaa)(H_2O)]_2[Ca(H_2O)_4]\}$ (**7**) with thermal ellipsoids at 30% probability.

Table 7. Selected Bond Lengths (Å) in the Complex $\{[Ca(tpaa)(H_2O)]_2[Ca(H_2O)_4]\}$ (**7**)

Ca(1)−N(1)	2.542(1)	Ca(1)−O(3)	2.468(1)
Ca(1)−N(2)	2.603(1)	Ca(1)−O(4)	2.877(2)
Ca(1)−N(3)	2.593(1)	Ca(1)−Ca(2)	3.878
Ca(1)−N(4)	2.804(1)	Ca(2)−O(4)	2.407(2)
Ca(1)−O(1)	2.432(1)	Ca(2)−O(5)	2.399(2)
Ca(1)−O(11)	2.489(1)	Ca(2)−O(1)	2.531(1)
Ca(1)−O(21)	2.535(1)	Ca(2)−O(11)	2.518(1)

The Ca(1) ions are nine-coordinated by the seven donor atoms of the $tpaa^{3-}$ ligand, by the oxygen of a water molecule and by a bridging water molecule with an irregular geometry. The ligand picolinate arms wrap around the metal in a helical conformation. The Ca(2) ion is eight-coordinated by the O-donors of four water molecules and the four O-donors of the bidentate bridging carboxylates (O(11), O(1)) with a square antiprismatic geometry. The angle between the two square planes (O(1#), O(4), O(5), O(11#), mean dev 0.22 Å and O(1), O(4#), O(5#), O(11), mean dev 0.22 Å) is 0.2°. An analogous trinuclear structure was already found for the calcium complex of HP-DO3A [10-(2-hydroxypropyl)-1,4,7,-10-tetraazacyclododecane-1,4,7-triacetic acid)].[41]

In the $tpaa^{3-}$ complex, the mean Ca−N distance (2.63-(11) Å) is slightly shorter than the mean Ca−N distance found in the $dpaea^{2-}$ complex in spite of the larger coordination number while the mean Ca−O(carboxylate) is very similar (2.48(4)Å). This is in agreement with the presence of a stronger interaction between the calcium ion and the trianionic ligand with respect to the bis-anionic $dpaea^{2-}$ ligand.

Table 8. ^1H Chemical Shifts of H_2dpaea and H_3tpaa and their Lead Complexes in D_2O at 298 K and at 200 MHz (H_2dpaea) and at 400 MHz (H_3tpaa)

H_2dpaea	CH_3	CH_2	Ha/Hb	H^1	H^2, H^3
pD = 2	1.49	3.59	4.67	7.52	7.87
pD = 7	1.33	3.21	4.29	7.32	7.69
pD = 10	1.19	2.69	3.80	7.32	7.66

Pb:H_2dpaea	CH_3	CH_2	Ha	Hb	H^1	H^2	H^3
pD = 3.0	1.20	3.06	4.28	4.56	7.77	8.11	8.00
pD = 5.9	1.23	3.09	4.30	4.59	7.80	8.08	8.03
pD = 11	1.00	2.69	4.39		7.68	8.02	8.02

H_3tpaa	CH_2	H^3	H^4	H^5
pD = 2.5	4.64	7.78	8.03	8.10
pD = 8.5	4.00	7.55	7.66	7.64

Pb: H_3tpaa	CH_2	H^3	H^4	H^5
pD = 2.8	4.54	7.63	7.88	7.96
pD = 9.5	4.47	7.59	7.85	7.93

Solution Structure and Formation Constants. The ^1H NMR spectra of 1:1 water solutions of H_3tpaa and Pb^{2+} show in the pH range 2.8−9.5 the presence of only one set of signals with three resonances for the nine pyridine protons and one resonance for the six methylene protons (Table 8). These features are consistent with a C_{3v} symmetry of the solution species in which all chelating arms of tpaa are equivalent. This seems to indicate that the asymmetric structures observed in the solid state are disrupted in solution for all complexes to give C_{3v} symmetric species probably through rapid proton exchange. The similar values of the chemical shift found for all protons in the pH range 2.8−9.5 suggest the presence of one major species in solution containing a trideprotonated form of the ligand in agreement with the potentiometric data (see below). Moreover, the chemical shift equivalence of the methylene protons requires a conformational mobility of the ligand branches in solution. The ^1H NMR spectra of 1:1 water solutions of H_2dpaea and Pb^{2+} in the pH range 3−6 shows the presence of only one set of signals with three resonances for the six pyridine protons and two resonances for the four methylene protons adjacent to the picolinate groups and two resonances for the ethyl group (Table 8). These features are in agreement with the presence of C_2 symmetric solution species in which the ligand remains bound to metal on the NMR time scale. The

more rigid coordination of the $dpaea^{2-}$ ligand, with respect to the $tpaa^{3-}$ ligand evidenced by the diastereotopicity of the methylene protons, suggests that the dipodal architecture is more adapted to lead binding than the tripodal one. At high pH (11), only one signal is observed for the methylene protons indicating the formation of different solution species probably due to hydroxide binding. At lower pH (1.6), the ^1H NMR spectrum of 1:1 water solutions of H_2dpaea and Pb^{2+} shows broad peaks in agreement with the presence of several species in slow exchange. This exchange involves most likely mono- and diprotonated species in solution in agreement with the isolation at this pH of the lead complex of the monoprotonated ligand. Below pH 0.5 (pH adjusted with a 10 M HCl solution), the spectrum shows only the presence of free protonated ligand which slowly precipitates out. The metalation and demetalation processes are very fast and occur immediately after pH adjustment indicating the possibility of reversible complexation of lead by the H_2dpaea ligand.

The proton NMR spectrum of 1:1:1 10^{-2} M water solutions of $Ca^{2+}/Pb^{2+}/H_2dpaea$ at pH 6 shows only the presence of one set of signals assigned to the lead complex in agreement with a higher affinity of the H_2dpaea ligand for the lead ion with respect to calcium.

The formation of the calcium and lead complexes with the H_2dpaea and H_3tpaa ligands was then investigated further with a potentiometric study.

H_3tpaa displays a low solubility in water at low pH (10^{-3} M); however, at pH > 7 deprotonation occurs and the solubility increases. The protonation constants of $tpaa^{3-}$, defined as $K_{ai} = [tpaaH_i]/[tpaaH_{i-1}][H^+]$, were previously reported to be $pK_{a4} = 2.5(2)$, $pK_{a3} = 3.3(1)$, $pK_{a2} = 4.11(6)$, and $pK_{a1} = 6.78(4)$ (0.1 M KCl, 298 K). NMR studies showed that the three first proton associations occur at the carboxylate functions, while the fourth protonation takes place at the apical tertiary amine nitrogen. The potentiometric titration of H_3dpaea^+ is indicative of two fairly strongly acidic sites and one weakly acidic site. The protonation constants of $dpaea^{2-}$, defined as $K_{ai} = [dpaeaH_i]/[dpaeaH_{i-1}][H^+]$, were determined to be $pK_{a3} = 2.6(1)$, $pK_{a2} = 3.5(1)$, and $pK_{a1} = 8.15(5)$ (0.1 M KCl, 298 K). The electron-withdrawing effect of the 6-methyl-2-pyridinecarboxylic acid groups significantly lowers the basicity of the tertiary amine. This effect is higher than for methylcarboxylic groups but lower than for methylpyridine groups. Indeed, the pK_a values of the apical amines range in the following order: dpa (bis(2-pyridylmethyl)amine, $pK_a = 7.30$) < dpaea ($pK_a = 8.15$) < ida (iminodiacetic acid, $pK_a = 9.34$) in the dipodal series. In the tripodal series, the order is as follows: tpa (tris(2-pyridylmethyl)amine, $pK_a = 5.98$) < tpaa ($pK_a = 6.78$) < nta (nitrilo-2, 2, 2″-triacetic acid, nta, $pK_{a2} = 9.65$).

The stability constants of the complexes formed between the Pb^{2+} ion and H_3tpaa or H_3dpaea have been determined by potentiometric titration of 1:1 metal/H_3tpaa and 1:1 metal/H_3dpaea mixtures in the pH range 2.2−8. Due to the insolubility of the [Ca(dpaea)] complex resulting in its precipitation at pH values greater than 5.7, its stability constant was determined by potentiometric titration of a 1:1 metal/H_3dpaea solution in the pH range 2.5−5.7. The titration curves of H_2dpaea and H_3tpaa and their Pb(II) and Ca(II) complexes are, respectively, shown in Figures 10 and 11.

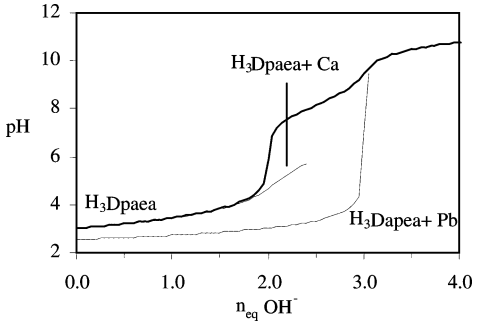

Figure 10. Alkalimetric titrations of solutions containing 10^{-3} M H_3Dpaea^+, 10^{-3} M $Ca^{2+}-H_3Dpaea^+$, and 10^{-3} M $Pb^{2+}-H_3Dpaea^+$ in water and 0.1 M KCl and at 298 K.

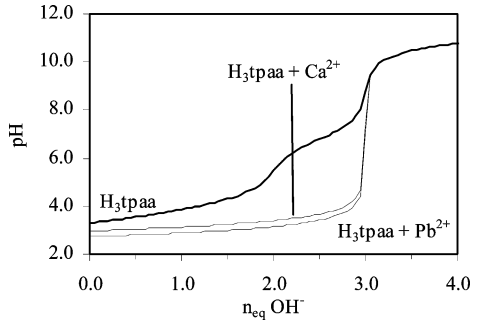

Figure 11. Alkalimetric titrations of solutions containing 0.5×10^{-3} M H_3tpaa, 0.5×10^{-3} M $Ca^{2+}-H_3tpaa$, and 0.5×10^{-3} M $Pb^{2+}-H_3tpaa$ in water, 0.1 M KCl, and 298 K.

Table 9. Stability Constants of Pb(II) and Ca(II) Complexes in Water at 298 K and $I = 0.1$ M (KCl)[a]

	tpaa	dpaea	edta[c]	tetam[d]
$\log \beta_{11}$(Pb)	10.0(1)	12.1(3)	18.0	8.29
$\log \beta_{11}$(Ca)	8.5(2)[b]	5.5(2)	10.65	2.62
Pb/Ca selectivity	$10^{1.5}$	$10^{6.6}$	$10^{7.35}$	$10^{5.67}$

[a] Log β_{11}, $\beta_{11} = [ML]/[M][L]$. [b] From ref 31. [c] From ref 37. [d] From ref 4.

Titration data could be fitted to eq 1, and the calculated equilibrium constants are reported in Table 9.

$$M + L \quad ML \quad \beta_{110} = [ML]/[M][L] \qquad (1)$$

Attempts to include partially protonated complexes did not result in any significant change of the fit, indicating that the partially protonated complexes isolated in the solid state are present in solution at very small concentration. Similarly, the potentiometric data do not indicate the presence of significant amounts of soluble hydroxide complexes of lead in the pH range 2.2−8.

The speciation diagrams presented in Figure 12 highlight the difference in the selectivities for lead over calcium of the two ligands $tpaa^{3-}$ ($10^{1.5}$) and $dpaea^{2-}$ ($10^{6.6}$). Pb^{2+} and Ca^{2+} complexes of $tpaa^{3-}$ are formed in the same pH range (pH ∼ 3−4). Conversely, the Pb^{2+} complex of $dpaea^{2-}$ is totally formed at pH 3.5 (99%) while only 0.3% of the total Ca^{2+} is bound in the same conditions.

Since the heptadentate ligand H_3tpaa and the pentadentate H_3dpaea contain exactly the same type of donor atoms, the

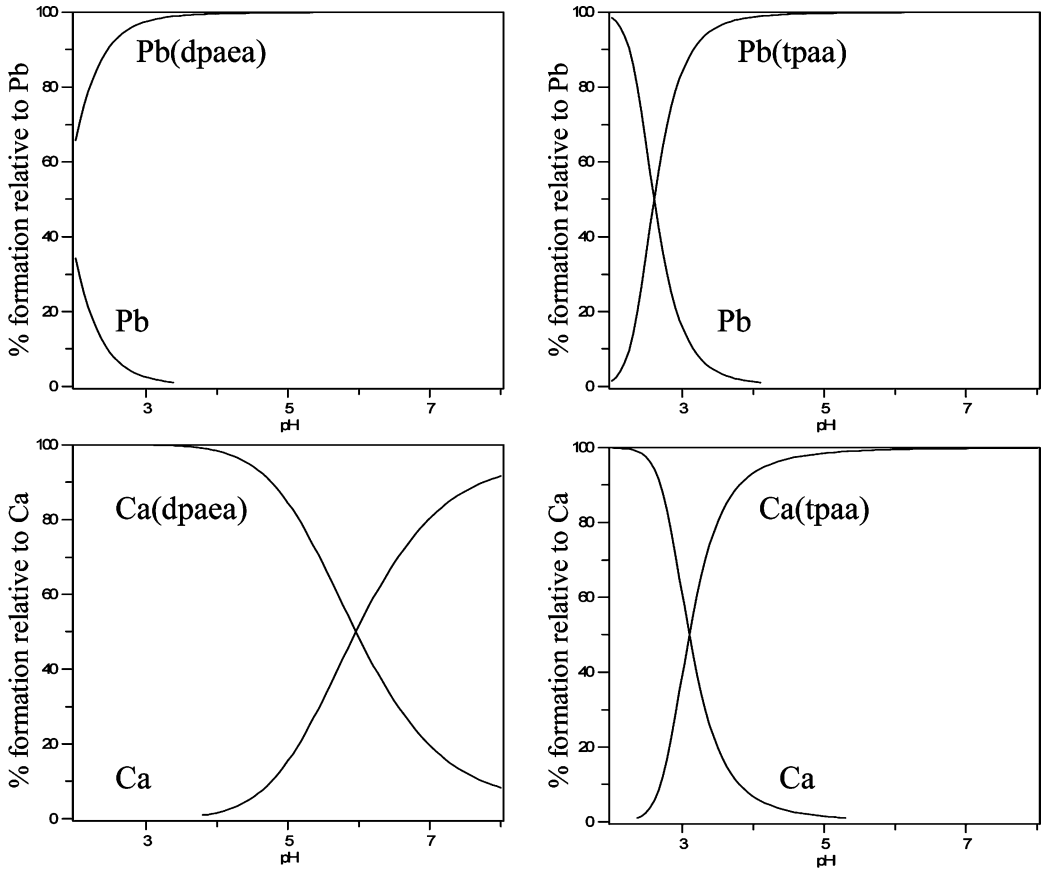

Figure 12. Lead and calcium speciation in the presence of $dpaea^{2-}$ and $tpaa^{3-}$. $[M^{2+}]_{tot} = [L]_{tot} = 10^{-3}$ M.

obtained data highlight the strong effect of the ligand geometry on the affinity for the lead ion and on the selectivity for lead over calcium. In spite of the higher negative charge and the larger number of donor atoms, a significantly lower stability is found for the $[Pb(tpaa)]^-$ complex with respect to the [Pb(dpaea)] one. Although divalent lead does not exhibit a preferential coordination geometry and tight binding is reported for both low denticity (4) and high denticity (6−8) ligands depending on the type of donor atoms, this is a rare example of lower stability observed for a ligand with higher denticity in the presence of the same type of donor atoms. The results presented here indicate a strong effect of the ligand architecture which can be explained by the ability of the $dpaea^{2-}$ geometry to better accommodate the lead lone pair. The increase of selectivity associated with the change in ligand geometry is remarkable; while the tripodal $tpaa^{3-}$ displays only a small Pb/Ca selectivity, the dipodal geometry leads to a high Pb/Ca selectivity, comparable or superior to extracting agents already used in lead removal from contaminated water and soils (see Table 9).

Conclusion

In this work, we have studied the complexation of lead and calcium by the tripodal picolinate ligand H_3tpaa and by the new dipodal ligand H_2dpaea designed to better accommodate the lead lone pair. The potentiometric study shows an important increase in the formation constant of the lead complex for the dipodal ligand with respect to the tripodal one, while a significant lower stability is found for the Ca(II) complex of $dpaea^{2-}$ with respect to the $[Ca(tpaa)]^-$ complex. This results in a dramatic increase of Pb^{2+}/Ca^{2+} selectivity for the dipodal ligand. The lower stability of the $dpaea^{2-}$ complex of calcium can be interpreted straightforwardly in terms of the lower charge and lower denticity of the H_2dpaea ligand. However, it is not possible to explain the higher stability of the Pb(II) complex of $dpaea^{2-}$ in terms of the nature of donor atoms which are very similar for the two ligands or of the complex overall charge, and only the different ligand geometry can account for the difference in stability. Indeed, the high value of the formation constant measured for the lead complex of $dpaea^{2-}$ ($\log \beta_{11}(Pb) = 12.1(3)$) compared to the lower value found for the one of the tripodal $tpaa^{3-}$ ($\log \beta_{11}(Pb) = 10.0(1)$) provides direct evidence of the influence of the stereochemically active lead lone pair on complex stability. As a result, since the ligand geometry has little effect on the stability of the calcium complex, a remarkable increase in the Pb/Ca selectivity is observed for $dpaea^{2-}$compared to $tpaa^{3-}$. The solid-state structures of the different isolated lead complexes provide evidence of the important structural effects of the lone pair of lead(II). Lead complexes containing protonated forms of H_2dpaea and H_3tpaa ligands were isolated. The potentiometric study shows that these are minor solution species in the pH range 2.2−8, and they are probably intermediate species in the metalation and demetalation processes. The crystal structures of the lead complexes of the diprotonated and monoprotonated tpaa show that the three picolinate arms of the tripodal ligand coordinate the lead in an asymmetric way

leaving a gap in the coordination sphere to accommodate the lead lone pair. As a consequence of this binding mode, one picolinate arm is very weakly bound (with very long Pb−N and Pb−O distances) and therefore can be expected to contribute very little to the complex stability in this intermediate species. Conversely, the structure of the lead complex of the monoprotonated $Hdpaea^-$ and diprotonated $dpaea^{2-}$ shows that all the ligand donor atoms are strongly bound to the metal ion. Since lead(II) would have a preference, according to the VSEPR theory, to adopt a linear coordination geometry where one of the coordination sites is occupied by the lead lone pair, higher stability should be expected for ligands that occupy only the site opposite to the lone pair.[16] The results presented in this paper provide direct evidence of the stereochemical activity of the lead lone pair on stability. In fact, in the structure of the [Pb(dpaea)] complex the donor atoms of the dipodal ligand occupy only a quarter of the coordination sphere, reducing the sterical interaction between the lead lone pair and the ligand and therefore leading to increased stability.

The high water solubility of the new dipodal ligand $dpaea^{2-}$, the fast metal complexation and demetalation, the reversible binding at low pH allowing for the total recuperation of the ligand in its original form, and the high selectivity for lead over calcium (3.9×10^6) which largely overcomes the typical 1:1000 concentration ratio typically found in drinking water contaminated by lead plumbing, make $dpaea^{2-}$ a very good candidate for application as an extracting agent for the lead removal from contaminated drinking water. Furthermore, the facile fonctionalization of H_2dpaea makes it very suitable for the development of new extracting materials for water purification processes by, for example, ligand grafting onto a silica surface.[4]

Acknowledgment. This work was supported by the Commissariat à l'Energie Atomique, Direction de l'Energie Nucléaire. We thank Christelle Gateau for useful discussions and ligand synthesis.

Supporting Information Available: Complete tables of crystal data and structure refinement, atomic coordinates, bond lengths and angles, anisotropic displacement parameters, hydrogen coordinates for compounds **1**−**7**. This material is available free of charge via the Internet at http://pubs.acs.org.

IC061823D